

# We are IntechOpen, the world's leading publisher of Open Access books Built by scientists, for scientists

5,300

Open access books available

132,000

International authors and editors

160M

Downloads

Our authors are among the

154

Countries delivered to

TOP 1%

most cited scientists

12.2%

Contributors from top 500 universities



WEB OF SCIENCE™

Selection of our books indexed in the Book Citation Index  
in Web of Science™ Core Collection (BKCI)

Interested in publishing with us?  
Contact [book.department@intechopen.com](mailto:book.department@intechopen.com)

Numbers displayed above are based on latest data collected.  
For more information visit [www.intechopen.com](http://www.intechopen.com)



# The Use of Avalanche Photodiodes in High Energy Electromagnetic Calorimetry

Paola La Rocca<sup>1,2</sup> and Francesco Riggi<sup>2</sup>

<sup>1</sup>*Museo Storico della Fisica e Centro Studi e Ricerche "E.Fermi"*

<sup>2</sup>*Department of Physics and Astronomy, University of Catania  
Italy*

## 1. Introduction

Avalanche Photodiodes (APD) are now widely used for the detection of weak optical signals. They find applications in a large number of fields of science and technology, from physics to medicine and environmental sciences. The request for sensitive detectors, capable to respond to weak radiations emitted from scintillation materials, has produced over the last decades an increasing number of studies on avalanche photodiodes and their applications as photo-sensors in particle detection. The first APD prototypes were developed more than 40 years ago. The initial size of such devices was however very small (below 1 mm<sup>2</sup>) and their spectral response confined to the near-infrared region. As a result, although available since several years, they did not receive much attention, also because of their initial high cost and low gain. However, large progresses have been made since then, and it has been possible to design and produce, at a reasonable cost, devices which have now a much larger area (tens of squared millimetres), with a high spectral sensitivity in the blue and near ultra-violet wavelength region. For such reasons, avalanche photodiodes are now widely used as sensitive light detectors in the construction of particle detectors in high energy physics. One of such examples is the impulse received by the design and construction of large scale electromagnetic calorimeters for the high energy experiments currently running in the world largest Laboratories. At present, APDs exhibit excellent quantum efficiency, with values around 80% in the near ultra-violet range, dropping to about 40% in the blue region, which is to be compared to typical values of 5-8 % in the blue for standard photomultipliers. Additional advantages which make them preferable over photomultipliers are discussed more specifically in the Chapter.

The overall set of problems and solutions related to the use of Avalanche Photodiodes in the design, construction, test and operation of large electromagnetic calorimeters in nuclear and particle physics experiments, is described in this Chapter, as observed within a Collaboration at the CERN Large Hadron Collider. Section 2 briefly recalls the principles on which electromagnetic calorimetry for particle physics experiments is based. Relative merits of Avalanche Photodiodes in comparison to traditional devices, mostly photomultipliers, are discussed in Sect.3, in connection with the light collection from scintillation detectors and the readout and front-end electronics. A review of the large detectors which have employed in the recent past or are currently employing such devices as photo-sensors is given in Section 4. Sect.5 describes the overall set of procedures carried out to characterize a large

number of such devices when installing a complex detector. Section 6 discusses also the problems which may be encountered in the digital treatment of the signal and presents a comparison between traditional and alternative approaches in the analysis procedures.

## 2. High energy electromagnetic calorimetry in nuclear and particle physics

The use of avalanche photodiodes in nuclear and particle physics has largely increased in the last decades especially in connection with the growing impact of calorimetry techniques on accelerator-based physics experimentation being taken in the world largest Laboratories. The term “calorimetry” comes from the Latin word *calor* (= heat) and indicates the basic detection principle which calorimeters are based on: the incident particles to be measured are fully absorbed in a block of instrumented material and their energy is converted into a measurable quantity (usually charge or light). In the process of absorption showers of secondary particles are generated, causing a progressive degradation in energy and producing some signal which can be detected to gain information on the original energy of the particle.

In order to match the physics potential at the major particle accelerator facilities, a wide variety of possible solutions for calorimeters is today available. Apart from the broad distinction between electromagnetic and hadronic calorimeters, they can be further classified according to the various types of technology employed, sampling calorimeters and homogeneous calorimeters being the most commonly used. This Chapter will focus on the electromagnetic calorimetry, describing the working principle and the practical realizations of electromagnetic calorimeters, as well as the reasons that make such detectors so attractive in the field of nuclear and particle physics. The interested reader is referred to textbooks (Wigmans, 2000) or review papers (Fabjan, 2003) for a more detailed discussion on calorimeters.

### 2.1 Working principle of an electromagnetic calorimeter

The various interaction mechanisms by which particles of different nature lose their energy in the medium underlie the broad distinction between hadronic and electromagnetic calorimeters: whereas hadronic calorimeters are built in order to exploit mostly the *strong* interactions experienced by hadrons (particles containing quarks, such as protons and neutrons) traversing matter, electromagnetic calorimeters detect light particles (electrons and photons) through their *electromagnetic* interactions with the medium's constituents.

Unlike hadronic showers, which are the result of a number of complex hadronic and nuclear processes, the physics of the electromagnetic showers is quite well-understood since it is based on few elementary processes, depending on the nature and energy of the incident particles. More precisely, *bremsstrahlung* and electron *pair production* are the dominant processes for high-energy electrons and photons: above 100 MeV electrons and positrons radiates photons (process called *bremsstrahlung*) as a result of the interaction with the nuclear Coulomb field; on the other hand, in the same energy range, photon interactions produce mainly electron-positron pairs. As a consequence, electrons and photons of sufficient high energy incident on a block of material create secondary photons and electron-positron pairs, which may in turn produce other particles through the same mechanisms. The result is a shower that may consist of thousands of different particles with progressively degraded energies. A diagram of an electromagnetic shower initiated by an electron is shown schematically in Fig 1.

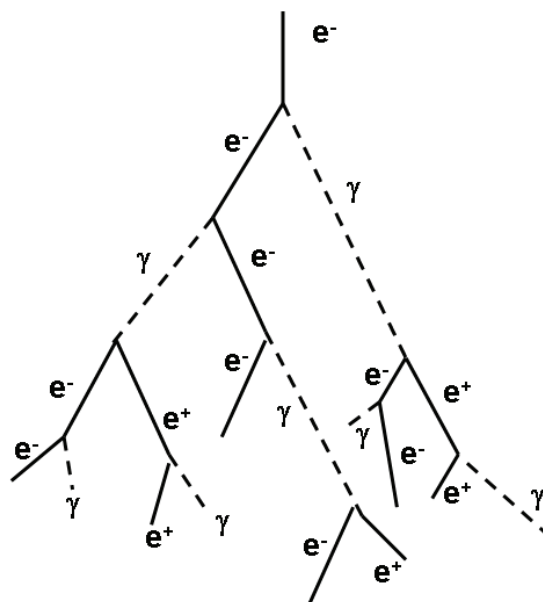


Fig. 1. Schematic diagram of an electron initiated electromagnetic shower.

This multiplication process is arrested when the energy of the secondary electrons produced in the electromagnetic cascade falls below a critical energy  $\epsilon$ , which may be defined as the energy at which the average energy losses from bremsstrahlung equal those from ionization. At this energy the electrons and positrons lose their energy through collisions with atoms and molecules of the absorber medium, causing ionizations and thermal excitation, while photons are more likely to lose their energy through Compton and photoelectric interactions. When the critical energy is reached, the shower contains the maximum number of particles; the depth at which this occurs is called *shower maximum*.

Since calorimeters have to measure the energy lost by particles that go through them, they are usually designed to entirely stop or absorb the incident particles, forcing them to deposit most of their energy within the detector. Depending on the particular construction technique, the energy lost by the incident particles is collected in the form of light or charge, producing a physical signal proportional to the amount of energy deposited.

All the energy loss mechanisms that characterize an electromagnetic shower can be calculated with a high degree of accuracy through Quantum Electrodynamics (QED) calculations. For this reason the main features of electromagnetic showers are well known and both the longitudinal and lateral profiles of the showers may be parameterized with simple empirical functions in terms of two parameters, the radiation length  $X_0$  and the Molière radius  $\rho_M$ . The first is defined as the mean distance over which a high-energy electron loses all but  $1/e$  of its energy by bremsstrahlung or, in case of photons, as  $7/9$  of the mean free path for pair production. The radiation length only depends on the characteristics of the traversed material and it is used to describe the longitudinal development of the shower in a material-independent way. On the other hand the second parameter, the Molière radius, is a measurement of the transverse size of a shower. More precisely it is the average lateral deflection of electrons at the critical energy after traversing one radiation length. The theoretical background needed for understanding the principle which electromagnetic calorimeters are based on is of great help for the evaluation of the performance characteristics of a real electromagnetic calorimeter, especially during the designing phase. The size, the construction principles and the materials used for an

electromagnetic calorimeter may be accurately chosen according to the environment in which it has to operate and the tasks it has to fulfil. Calorimetry is the art of compromising between conflicting requirements, such as the energy and spatial resolution, the triggering capabilities, the radiation hardness of the materials used, the dynamic range and so on. Some more details about these aspects will be given in the following sections, together with some practical details of building and operating these detectors.

## 2.2 Homogeneous and sampling calorimeters

From the construction point of view, the possible solutions for calorimeters is very wide and quite ingenious calorimeter systems have been designed to cope with more and more demanding physics goals and requirements.

Here we will divide calorimeters only in two broad categories, sampling and homogeneous calorimeters.

### Sampling Calorimeters

Sampling calorimeters consist of layers of *passive* or *absorber* high-density material (lead for instance) interleaved with layers of *active* medium such as solid lead-glass or liquid argon. Absorber layers are used to enhance photon conversions, while active layers to sample energy loss.

The main drawback of these devices is their limited energy resolution which rises from the large fluctuations, caused by the absorbers, in the energy deposited in the active layers. On the other hand, their excellent space resolution (i.e. their capability to reconstruct the impact position of incident particles) and their satisfactory particle identification are the result of the laterally and longitudinally segmentation, that is relatively easy to implement.

Many types of sampling calorimeter exist, which differ one another in the type of materials used. The most common absorber materials are lead, copper and iron, while the active medium can be solid (scintillator and semiconductor), liquid or gaseous.

In sampling calorimeters the energy deposited by showering particles can be collected both in the form of light, as in case of scintillation calorimeters, and in the form of electric charge, as happens in gas, solid-state and liquid calorimeters. Some details about the techniques used to collect the light signal are given in Section 3.1.

### Homogeneous Calorimeters

In homogeneous calorimeters the same medium is used both to cause the shower development and to detect the produced particles. As discussed later, the main advantage of these devices is their excellent energy resolution, since the intrinsic fluctuations that occur in the development of the showers are small with respect to sampling calorimeters.

Usually homogeneous calorimeters are difficult to be segmented and this reduces their capabilities to give information about the position of the incident particle and its identification.

Since the materials used to build homogeneous calorimeters are characterized by large interaction lengths, such devices are almost exclusively used for electromagnetic calorimetry. Homogeneous calorimeters can be classified, according to the type of active material, into semiconductor calorimeters, noble-liquid calorimeters, Cherenkov calorimeters and scintillator calorimeters. Whereas the first two types of devices are based on the charge measurement, in scintillator and Cherenkov calorimeters the signal is collected in the form of light: the photons produced are converted into electrons and the electric signal is amplified to reduce the



electronic noise level. This is usually performed by photo-sensitive devices, such as photomultipliers, which are able to reach multiplication gains of the order of  $10^6$ . However, the use of magnetic fields in modern particle experiments prevents the use of traditional photomultipliers: in these cases avalanche photodiodes are a valid alternative; however they provide a moderate gain, causing a non negligible noise term.

The choice of the typology and of the detector parameters for a specific application depends on several factors, such as the physics goals, the energy range that has to be considered, the accelerator characteristics and the available budget as well. Often the choice is supported by results from tests of small prototypes with particles beams, as well as by detailed simulation studies of the calorimeter performance.

### 2.3 The energy response of a calorimeter

In an electromagnetic calorimeter, the energy dissipated by the charged particles of a shower in the detector material is converted into a detectable signal which provides information on the original energy of the incident particle. This is verified both in case of homogeneous and sampling calorimeters: in the former, the whole energy of an incident particle is deposited in the active material, so that the entire detection volume may contribute to the signals that the particle generates; in the latter, the presence of passive absorber layers reduces the energy lost in the active layers to a fixed fraction (called sampling fraction) of the original energy.

However, the energy response of calorimeters depends on the nature of the incident particle: whereas showering electrons and photons produce a signal that is proportional to the original energy, the same is most certainly not valid for hadrons because part of their energy is used to dissociate the atomic nuclei and does not contribute to the calorimeter signals. Hence, the hadronic signals from electromagnetic calorimeters are non-linear and are not constant as a function of energy. In the following we will focus exclusively on the response of electromagnetic calorimeters to electron and photons.

In order to provide a reliable measurement of the energy, a first requirement that has to be fulfilled concerns the containment of the shower inside the detector volume. As the energy of the incident particle increases, the detector size needed to contain the showers increases as well. For electromagnetic showers, a simple formula that gives approximately the location of the shower depth expressed in radiation lengths is the following:

$$x_{\max} \approx \ln(E/\varepsilon) + x_0 \quad (1)$$

where  $E$  is the energy of the incident particle, and  $x_0 = 0.5$  for photons and  $-0.5$  for electrons. This expression shows that the longitudinal size of a shower increases only logarithmically with energy, allowing to design a compact detector even for electromagnetic showers depositing a large energy (hundred of GeV) into the sensitive volume. On the other hand, the thickness containing 95% of the total shower energy is approximately located at  $x_{95\%} \approx x_{\max} + 0.08Z + 9.6$ , indicating that the realization of compact calorimeters requires the use of high- $Z$  materials.

Therefore, even at the particle energies reached at the Large Hadron Collider, electromagnetic calorimeters are very compact devices and energetic showers lose only a small percentage of their energy beyond the end of the active calorimeter volume.

Besides being intrinsically linear, electromagnetic calorimeters should also give a precise measurement of the energy. The precision with which the unknown energy of a given

particle is measured is called *energy resolution* and represents one of the most important performance characteristics of a calorimeter.

The actual energy resolution of a realistic electromagnetic calorimeter can be in general parameterized as follows:

$$\sigma/E = a/\sqrt{E} \oplus b/E \oplus c \quad (2)$$

where  $\sigma$  is the standard deviation in the energy measurement, the constants  $a$ ,  $b$  and  $c$  depend on the detector characteristics and the symbol  $\oplus$  indicates a quadratic sum.

From the left-hand side, the three terms are known as *stochastic term*, *noise term* and *constant term* respectively; the importance of each term strongly depends on the energy deposited in the calorimeter.

The stochastic term arises from the shower intrinsic fluctuations that characterize electromagnetic cascade developments event by event. Unlike homogeneous calorimeters, where these fluctuations are moderate, the stochastic term is quite important especially in sampling calorimeters, due to the presence of the absorber layers.

The noise term arises from the electronic noise of the readout chain. Usually it does not weight much upon the total energy resolution, especially for calorimeters in which the signal is collected in the form of light because, in that case, the first step of the electronic chain is a photo-sensor (like a phototube or a Silicon photomultipliers) which amplifies the original signal with almost no noise.

However, for energetic particles as those produced in the new-generation accelerators, the dominant contribution to the energy resolution is the constant term, that does not depend on the energy of the particle and arises from systematic effects (such as detector non-uniformities, shower leakage, mis-calibration,...). Therefore, modern calorimeters are built imposing severe construction tolerances in order to reduce possible instrumental imperfections that may give rise to response non-uniformities.

Additional contributions can make the energy resolution of a calorimeter worse, such as lateral and longitudinal leakages of the energy shower outside the active calorimeter volume, or fluctuations due to energy losses of electrons and photons in inactive materials (mechanical structures and cables) before reaching the calorimeter. These effects mainly affect the energy resolution of calorimeters integrated in complex high-energy physics experiments where the calorimeter is only one component that has to satisfy several mechanical constraints.

#### **2.4 The tasks of an em-calorimeter**

Calorimeters were originally conceived as devices used to measure only the energy of the incident particles. Today they have different applications and often their tasks are made more effective when the information they provide is combined with that coming from other sub-detectors.

The reasons that make calorimeters so attractive are various. First of all they provide a precise measurement of the energy in a wide range, since the energy resolution varies with energy as  $1/\sqrt{E}$ . This characteristic is crucial when looking for narrow resonances characterized by a poor signal/background ratio, as in the case of the search for Higgs bosons decaying into  $\gamma\gamma$ . Moreover, the capability to entirely absorb high energetic showers in compact distances make electromagnetic calorimeters the suitable instrument to measure electrons and photons over an unprecedented energy range, as requested by the experiments running at recent accelerator facilities like the LHC.

Electromagnetic calorimeters can also provide a fairly good particle identification, being able to distinguish, for instance, electrons and photons from muons and pions on the basis of their different energy deposit profiles. Moreover, calorimeters are sensitive to all kind of particles, including neutral ones. This feature is particularly exploited in particle physics experiments for several applications: for example, when measuring jets of particles (i.e. the characteristic collimated sprays of hadrons coming from hard collisions between energetic partons), electromagnetic calorimeters can give a measurement of the neutral component of the jets, completing the information provided by other kinds of detectors sensitive only to charged particles. Moreover, in modern experiments, calorimeters are built in order to have an angular coverage as large as possible, achieving often hermeticities in excess of 90%; in this way they can provide an indirect measurement of weakly interacting particles, as neutrinos, that can be detected only by observing geometric imbalances (missing energy) in the total transverse energy.

The possibility to segment electromagnetic calorimeters into several identical cells allows to gain information also on the impact position of the incident particles. The shower position is determined by reconstructing the centre of gravity of the energy deposited in the various detector cells that contribute to the signal. The precision with which the position of a given particle is measured mainly depends on the granularity of the detector and can achieve accurate values. The granularity of an electromagnetic calorimeter plays also an important role for the minimization of the *pileup* phenomena, i.e. the overlap of signals coming from different particles hitting the same cell. This problem may occur in calorimeters running in high-density particle environments characteristic of ultra-relativistic heavy-ion collisions. Moreover, the high luminosities achieved in modern hadron colliders may cause another type of pileup due to the overlap of signals coming from the preceding or following bunch crossing. To avoid event overlaps the calorimeter response in time is usually fast enough. This important feature is extensively used to select or trigger on interesting events, especially in those experiments in which the event rate is orders of magnitude beyond the rate at which events may be collected by the data acquisition system. Signals from calorimeters are available at very short time after the particle impact and are easy to process and interpret: the characteristics derived from the calorimeter data allows physicists to select only interesting (and often rare) events, such as those containing jets of particles or very energetic electrons and photons.

Thanks to all these features, calorimeters became key components of particle detectors and today almost every experiment in particle physics relies heavily on calorimetry.

### **3. Readout systems based on Avalanche Photodiodes: problems and solutions**

#### **3.1 Light collection in electromagnetic calorimeters**

In order to collect all the energy deposited in each calorimeter cell, a proper readout system must be designed, to convert the light produced in the active material into an electronic signal which can be handled by the analog-to-digital converters and/or used by the trigger logic. Any readout system must be designed in such a way not to disturb the working condition of the calorimeter. For instance, no additional effect has to be introduced as far as the energy, position and time resolution are concerned. Moreover, the hermeticity of the calorimeter needs not be degraded by the readout part of the detector, as well as the overall radiation hardness.



In case of homogeneous calorimeters, which usually consist of individual crystals, scintillation or Cerenkov light is generated by the passage of particles. Each crystal is read out from the back, by the use of a photomultiplier tube (PMT) or by a different light sensor. While traditional readout devices employed photomultipliers in the past, solid-state devices started to be used more than 15 years ago. Silicon photodiodes (Barlow et al., 1999), Hybrid Photon Detectors (Anzivino et al., 1995) or APDs (Lorenz et al., 1994) are among the oldest examples of such devices.

Sampling calorimeters have been used since the very beginning in particle physics. In these structures, metal plates are interleaved with active scintillation materials. The geometry of the first generation calorimeters was very simple, with the scintillation light being extracted by each scintillation portion of the detector, coupled to one or two photomultipliers. In recent years however, the geometry of sampling calorimeters has changed considerably, mainly to design calorimeters with hermeticity properties. The development of wavelength shifting WLS fibers has allowed to design calorimeters with a fine segmentation of the active material, without enlarging the number of readout channels. In sampling calorimeters, the WLS fibers run along the length of each cell or perpendicular to it, and all the portions of the scintillation material are optically coupled to a photon detector located behind the calorimeter. This has the advantage that all the active parts of a cell are read out by the same photo-sensor. Some disadvantages inherent to this technique are related however to the worsening of the signal timing, which is much slower than that of the scintillation process, and to the partial non-hermeticity introduced by the volume itself of the WLS fibers. The latter may be solved with the use of scintillating and wavelength shifting fibers.

As far as the time structure of the signal is concerned, the absorption of the electromagnetic shower induced in a calorimeter by a high energy particle or radiation takes a time in the order of a few nanoseconds, due to the typical size of each individual module. However, the detection of neutrons has a much longer time scale, since they may be scattered from the surrounding materials. As a consequence, a long tail may be observed, which also requires some intervention on the associated electronics, such as to modify the shaping time of the signal in order to cut a large fraction of this tail.

In addition to the late arrival of neutrons, other instrumental effects may also have their influence on the time structure of the signals. One of these effects is due to the nature of the particular scintillation material used as active element in the calorimeter, since the fluorescent processes by which light is produced inside a scintillation material have characteristic decay times which range from nanoseconds to milliseconds. While organic scintillators have decay times of a few nanoseconds, considerably longer times (300 ns) are typical of BGO material.

An important aspect to be considered in understanding the time structure of the signal - especially for large volume calorimeters - is the fact that relativistic particles which produce the light inside the scintillation detector cover the distance between the front face of the detector and the photo-detector in a time which is smaller than the time required to the light photons produced by their passage, due to the refraction index  $n$  of the material. Such difference between  $c$  and  $c/n$  may amount to a few nanoseconds, which may be relevant in case of fast scintillators.

### **3.2 Avalanche Photodiodes as photo-sensors in calorimeters**

Silicon Avalanche Photodiodes are now considered good candidates to replace traditional photomultipliers to detect the light produced in scintillation materials, especially in specific

situations, where their advantages become more apparent. APDs have several features which make them attractive for scintillation detection. The discussion of the working principles of such devices and their detailed structure is beyond the scope of the present Chapter. Here only follows a list of different aspects which are relevant for the use of APDs as photo-sensors in electromagnetic calorimeters, and which need to be evaluated when choosing the proper solution:

**Size:**

Photomultipliers have different sizes, which can be adapted in principle to any specific situation. However, the size of traditional photomultipliers is always much bigger than their sensitive area, which can be a problem for large detector arrays, as it is the case with large particle detectors. On the contrary, APDs have limited sizes (in the order of a 1-50 mm<sup>2</sup>) and the required front-end electronics may also be very compact. For such reasons, their use is suitable to the need of a large granularity crystal array (in case of homogeneous or sampling calorimeters). On the other side, their small size may require sometimes to employ more than one device per crystal, in order not to reduce too much the amount of collected light.

**Internal gain**

APDs are components which possess an intrinsic internal gain. The applied bias voltage produces a region where a high electric field (in the order of 150 kV/cm) is obtained. Such field is able to generate avalanches of secondary particles, and hence to amplify the signal. The exact value of the internal gain coefficient depends on the applied bias voltage and also on the temperature. In comparison to the possibility of "external" gain, the intrinsic gain has the advantage of using all the signal generated by the light development inside the scintillation crystal, whereas the signals generated within the sensitive volume of the diode are not amplified.

**Insensitivity to magnetic field**

Due to the need to bend charged particles emitted in a nuclear collision and hence measure their momentum according to the curvature of the track, a large fraction of a modern particle detector is usually contained inside a magnetic field. Large magnetic fields, up to several Tesla, may be in order, with the aim to bend very energetic (GeV or more) particles. Such fields however do not allow the use of traditional photomultipliers, since electron trajectories would be highly distorted by the field, and even robust shielding could be ineffective to protect them. Moreover, the use of a thick shielding would cause a large number of secondary interactions in the material, which could be of disturb for the detection of particles and radiations in the active detectors. The use of traditional PMTs would then require to transport the light through optical fibers for a long distance outside the magnetic field. APDs on their side are not sensitive to magnetic fields, which makes them the device of choice for particle detectors embedded in large magnets.

**Spectral response**

While the spectral response of an Avalanche Photodiode is nearly the same as for a normal photodiode when no bias is applied, this changes as a result of the application of the bias voltage, since the penetration depth of the light inside the device depends on the wavelength. Devices which have an enhanced sensitivity in the near-infrared region or at smaller wavelengths (300 nm) are available nowadays, to allow the user to select the appropriate device.

### **Quantum efficiency**

The overall efficiency of a photo-sensor strongly depends on how good is the matching between the emission spectrum of the scintillation material being used and the spectral response of the photosensor. Avalanche photodiodes usually exhibit a very high quantum efficiency (QE), relatively constant over a wide wavelength interval. As an example, the APDs employed in the ALICE and CMS calorimeters exhibit a quantum efficiency of the order of 85% from 500 to 800 nm, dropping down to 50% at 350 and 950 nm. These values are significantly higher than the average values for standard photomultipliers, which are in the order of 20%.

### **Gain stability**

The gain of an Avalanche Photodiode depends both on the applied voltage and on the temperature, so it is important to measure, for any individual APD, the relevant coefficients, in order to allow for possible variations in these quantities. The stability of the bias voltage depends on the overall quality of the power supply and (to some extent) on the environmental conditions. While it is not so critical to control the bias voltage, a relevant problem is that the gain of each APD needs to be individually adjusted to match a common value of the gain, which requires a software-controlled power supply, able to distribute to each APD channel the appropriate voltage. Concerning the temperature dependence, this is an important factor to maintain the gain stable over time, since the ambient temperature may be subjected to non negligible variations over long time operational periods. Moreover, due to the large number of channels usually involved, sensible temperature differences are experienced by devices which are located even meters apart, so that a monitoring and correction of the bias voltage to overcome such temperature-dependent gain variations is mandatory to equalize the gain in different channels.

Measurements have been also performed (Chartrchyan et al. 2008) on the long term stability of such devices, maintaining them under bias voltage for long periods, up to 250 days, and checking for possible failures through the monitoring of the dark current. Values of the MTTF (mean time to failure) of the order of  $10^7$  hours have been reported.

### **Negligible nuclear counter effect**

The nuclear counter effect is related to the amount of extra signal produced inside the photodiode by a charged particle traversing it, which adds to the charge produced by the scintillation light in the crystal. It can be quantified by the thickness of a Si PIN diode required to produce the same signal. The signal produced in the APD would be proportional to such equivalent thickness. From this point of view, the effective thickness of the device should be minimized as much as possible in order to reduce the influence of the nuclear counter effect. However, reducing the thickness has also the effect of increasing the APD capacitance, so that a compromise needs to be reached.

### **Small excess noise**

Avalanche photodiodes generate excess noise, due to the statistical nature of the avalanche process. An estimate of the statistical fluctuations of the APD gain is given by the excess noise factor  $F$ , where  $\sqrt{F}$  is the factor by which the statistical noise on the APD current exceeds that expected from a noiseless multiplier. The excess noise has its origin in the intrinsic statistical nature of the internal charge carrier multiplication inside the device, which depends on the inhomogeneities in the avalanche region and in hole multiplication. If

$k$  is the ratio of the ionization coefficients for electrons to holes, at a given gain  $M$ , the excess noise factor is given by:

$$F = k \times M + (2 - 1/M) \times (1-k) \quad (3)$$

The result is an additional contribution to the energy resolution, and clearly a small value of the excess noise factor is preferable to optimize the overall resolution. This factor increases with the gain, reaching for instance a value of about 1.9 at  $M=30$  for the APD employed in the ALICE and CMS calorimeters. Large area APDs which have been subsequently developed for the PANDA calorimeter, exhibit smaller values of  $F$  (1.38 at  $M=50$ ).

### High resistance to radiations

The use of Avalanche Photodiodes in hostile environments, as far as the radiation level is concerned, is a critical point for large particle physics experiments, where the flux of charged and neutral particles produced in high energy collisions over long operational periods may be very high. The dose absorbed by the detectors and associated electronics is usually evaluated by detailed GEANT simulations which take into account the description of the complex geometry and materials of the detector. Depending on the physics program (proton-proton or heavy-ion collisions, low or high beam luminosity, allocated beam time,...) and on the location of such devices inside the detector, a particular care must be devised to understand whether the photo-sensors will be able to survive during the envisaged period of operation. For such reason, a detailed R&D program has been undertaken within the High Energy Collaborations to expose the devices of interest to different sources of radiations, and measure their performance before and after irradiations. There are basically two damage mechanisms: a bulk damage, due to the displacement of lattice atoms, and a surface damage, related to the creation of defects in the surface layer. The amount of damage depends on the absorbed dose and neutron fluence.

Whereas experiments like ALICE, which will run with low luminosity proton and heavy ion beams at LHC, do not suffer of big problems with the radiation dose in the electromagnetic calorimeter, the CMS detector, which runs at a much larger luminosity, will have a very large dose in the photo-sensors. As an example, in ten years LHC operation, the planned dose in the CMS barrel is in the order of 300 Gy, with a neutron fluence of  $2 \times 10^{13}$  n/cm<sup>2</sup> (1 MeV-equivalent). This has led to an extensive set of measurements with different probes (protons, photons and neutrons), and to the successful development of APDs capable to survive to these conditions.

### 3.3 Front-end electronics

Once the light produced in the active material has been collected by the photosensor, an important step towards the extraction of the signal is the associated front-end electronics. Such electronics has to be used to process the signal charge delivered by the photo-sensors and extract as much information as possible concerning the time and amplitude of the signal. Several aspects are important to understand the requirements which are demanded to front-end electronics.

#### Dynamic range

In high energy experiments, for instance in the experiments running at LHC, the dynamic range required to a calorimeter is very high. Signals of interest go from the very small amplitudes associated to MIP particles (for instance, cosmic muons used for the calibration,

which typically deposit an energy of a few hundred MeV in an individual cell) to highly energetic showers (in the TeV region) produced by hadrons or jets. The dynamic range required may then easily cover 4 orders of magnitude, which requires a corresponding resolution in the digitization electronics (ADC with 15-16 bits). An alternative approach is the use of two separate high-gain and low-gain channels, which requires ADCs with a smaller number of bits, at the expense of doubling the number of channels.

### **Time information**

The extraction of timing information from the individual signals originating from each module in a segmented calorimeter is an important goal for the front-end electronics. Time information may be important in itself, also for calibration and monitoring purposes, and it is mandatory when the information from a calorimeter must be used to provide trigger decisions. The timing performance of the overall readout system also depends on the rest of the electronics, as well as on the algorithms being used to extract such information (See Sect.6).

### **Number of independent channels**

Due to the large granularity usually employed in segmented calorimeters, the number of independent channels is very high, in the order  $10^4$ - $10^5$ . This requirement demands a corresponding high number of front-end preamplifiers and a high level of integration for the associated electronics, which needs to be compacted in a reasonable space.

## **3.4 Monitoring systems**

A common aspect to all kind of detectors which are used to transform the light, produced in the active part of the calorimeter, into an electric signal, is the fact that their exact response (gain) is intrinsically unstable, depending on a number of factors which may vary according to the experimental conditions. Temperature and voltage variations are particularly important in this respect, as discussed before, since the gain of Avalanche Photodiodes is very sensitive to such parameters. Such aspects require usually a careful study of the devices being used, under the specific working conditions, in order to characterize their response as a function of these parameters (see Sect.5). Moreover, a monitoring system is in order, to take into account the variation of the working parameters, and sometimes even to correct the gain by a proper feedback. A LED monitoring system is usually employed in large calorimeters, with the aim to send periodically a reference signal to all readout cells and to check the response uniformity.

## **4. A review of large APD-based electromagnetic calorimeters**

Most of the large experiments devoted to high energy physics make use of calorimeters, to detect hadronic and electromagnetic showers originating from energetic particles and radiations. Electromagnetic calorimeters in particular are employed since several decades, making use in the past of traditional photo-sensors (photomultipliers) and, more recently, of solid-state devices such as photodiodes, APD and silicon photomultipliers. Here a brief review is given of several experiments in high-energy physics which have an electromagnetic calorimeter as an important part of the detection setup.

### **4.1 Calorimeters based on traditional photo-sensors**

Several high-energy experiments installed in the largest nuclear and particle physics Laboratories have employed in the past electromagnetic calorimeters of various



configurations and design, with traditional photomultipliers or photodiodes as photon sensitive devices. As an example, Table 1 shows a (non-exhaustive) list of detectors which include an electromagnetic calorimeter, together with some basic information on the organization and design of the detector. As it can be seen, the largest installations have a number of channels in the order of  $10^4$ , which is remarkable for traditional readout systems based on photomultipliers.

Experiment	Laboratory	Type	No.of channels
E731	FNAL	Lead Glass	802
CDF	FNAL	Lead/Scint	956
FOCUS	FNAL	Lead/Scint	1136
SELEX (E781)	FNAL	Lead Glass	1672
BABAR	SLAC	CsI (photodiode)	6580
L3	CERN /LEP	BGO Crystals (photodiode)	10734
OPAL	CERN /LEP	Lead Glass	9440
HERMES	DESY /HERA	Lead Glass	840
HERA-B	DESY/HERA	Pb(W-Ni-Fe)/Scint Shashlik-type	2352
H1	DESY/HERA	Lead-scintillating fibre	1192
ZEUS	DESY/HERA	Depleted uranium-Scint calorimeter, WLS	13500
WA98	CERN /SPS	Lead Glass	10080
KLOE	LNF	Lead-scintillating fibre	4880
STAR	RHIC	Pb/Scint Sampling calorimeter, WLS	5520
PHENIX	RHIC	Pb/scint shashlik-type	15552
PHENIX	RHIC	Pb glass	9216
LHCb	CERN /LHC	Lead/Scint shashlik-type, WLS	5952

Table 1. Summary of detector installations which make use of an electromagnetic calorimeter with traditional readout devices.

#### 4.2 Calorimeters making use of Avalanche Photodiodes

Only in the last years Avalanche Photodiodes have been routinely employed as photosensors for large electromagnetic calorimeter installations. Here we want to briefly summarize a few examples of recent detectors which have been installed and commissioned or in the stage of being constructed.

### **The electromagnetic calorimeter of the CMS experiment at LHC**

CMS (Compact Muon Solenoid) is one of the large experiments running at the CERN Large Hadron Collider (LHC). A general description of the CMS detector is reported in (Chartrchyan et al. 2008). A large electromagnetic calorimeter, based on lead tungstate crystals with APD readout, is included in the design of the CMS detector.

The barrel part of the CMS electromagnetic calorimeter covers roughly the pseudo-rapidity range  $-1.5 < \eta < 1.5$ , with a granularity of 360-fold in  $\phi$  and 2x85-fold in  $\eta$ , resulting in a number of crystals of 61200. Additional end-caps calorimeters cover the forward pseudo-rapidity range, up to  $\eta=3$ , and are segmented into 4 x 3662 crystals, which however employ phototriodes as sensitive devices.

The use of lead tungstate crystals with its inherent low light yield and the high level of ionizing radiations at the back of the crystals has precluded in this case to employ conventional silicon PIN photodiodes. In collaboration with Hamamatsu Photonics, an intensive R&D work has led the CMS Collaboration to the development of Si APDs particularly suited to such application (Musienko, 2002). As a result of this work, a compact device (5x5 mm<sup>2</sup> sensitive area, 2 mm overall thickness) has been produced, which is now used also by other experiments. The performances of such device are its fast rise time (about 2 ns) and the high quantum efficiency (70-80 %), at a reasonable cost for large quantities. To overcome the inherent limitations of a reduced gain at wavelength smaller than 500 nm, and a high sensitivity to ionizing radiation, an inverse structure for such devices was implemented. In these APDs the light enters through the p<sup>++</sup> layer and is absorbed in the p<sup>+</sup> layer. The electrons generated in such layer via the electron-hole generation mechanism drift toward the pn junction, amplified and then drift to the n<sup>++</sup> electrode, which collects the charge. The APD gain is largest for the wavelengths which are completely absorbed in the p<sup>+</sup> layer, which is only a few micron thick; as a result, the gain starts to drop above 550 nm. Moreover, with this reverse structure, the response to ionizing radiation is much smaller than a standard PIN photodiode.

An important issue for the APD installed in the CMS detector is the effect of radiation on the working properties of the device, due to high luminosity at which this experiment is expected to run for most of its operational time. In ten years of LHC running, the neutron fluence (1 MeV equivalent) in the barrel region is expected in the order of 10<sup>13</sup> n/cm<sup>2</sup>, with a dose of about 300 Gy. The extensive irradiation tests performed in the context of this Collaboration have provided evidence that the devices are able to survive the long operational period envisaged at LHC.

Due to the large area of the crystals employed in the CMS calorimeter, compared with the sensitive area of the APD devices, two individual Avalanche Photodiodes are used to detect the scintillation light from each crystal.

### **The electromagnetic calorimeter of the ALICE experiment at LHC**

The ALICE detector (Aamodt et al., 2008) is another large installation at LHC, mainly devoted to the heavy ion physics program. It is equipped with electromagnetic calorimeters of two different types: the PHOS (PHOton Spectrometer), a lead tungstate photon spectrometer, and the EMCAL, a sampling lead-scintillator calorimeter. These two detectors are able to measure electromagnetic showers in a wide kinematic range, as well as to allow reconstruction of neutral mesons decaying into photons.

The PHOS spectrometer is a high resolution electromagnetic calorimeter covering a limited acceptance domain in the central rapidity region. It is divided into 5 modules, for a total

number of 17920 individual Lead tungstate (PWO) crystals. Each PHOS module is segmented into  $56 \times 64 = 3584$  detection cells, each of size  $22 \times 22 \times 180$  mm, coupled to a  $5 \times 5$  mm<sup>2</sup> APD.

An additional electromagnetic calorimeter (EMCal) was added to the original design of ALICE, to improve jet and high-pt particle reconstruction. This is based on the shashlik technology, currently employed also in other detectors. The individual detection cell is a  $6 \times 6$  cm<sup>2</sup> tower, made by a (77+77) layers sandwich of Pb and scintillator, with longitudinal wavelength shifting fiber light collection. The total number of towers is 12288 for the 10 super-modules originally planned (which cover an azimuth range of 110°). Recently a new addition of similar modules started, to enlarge the electromagnetic calorimeter (DCAL), providing back-to-back coverage for di-jet measurements. This will roughly double the number of channels.

The active readout element of the PHOS and EMCal detectors are radiation-hard  $5 \times 5$  mm<sup>2</sup> active area Avalanche Photodiodes of the same type as employed in the CMS electromagnetic calorimeter. These devices are currently operated at a nominal gain of  $M=30$ , with a different shaping time in the associated charge-sensitive preamplifier.

#### **The electromagnetic calorimeter of the PANDA experiment at FAIR**

PANDA is a new generation hadron physics detector (Erni et al., 2008), to be operated at the future Facility for Antiproton and Ion Research (FAIR). High precision electromagnetic calorimetry is required as an important part of the detection setup, over a large energy region, spanning from a few MeV to several GeV. Lead-tungstate has been chosen as active material, due to the good energy resolution, fast response and high density. To reach an energy threshold as low as possible, the light yield from such crystals was maximized improving the crystal specifications, operating them at  $-25$  °C and employing large area photo-sensors. The largest part of such detector is the barrel calorimeter, with its 11360 crystals (200 mm length). End-cap calorimeters will have 592 modules in the backward direction and 3600 modules in the forward direction. The crystal calorimeter is complemented by an additional shashlyk-type sampling calorimeter in the forward spectrometer, with 1404 modules of  $55 \times 55$  mm<sup>2</sup> size.

The low energy threshold required of a few MeV and the employed magnetic field of 2 T precludes the use of standard photomultipliers. At the same time, PIN photodiodes would suffer from a too high signal, due to ionization processes in the device caused by traversing charged particles. In order to maximize the light signal, new prototypes of large area ( $10 \times 10$  mm<sup>2</sup> or  $14 \times 6.8$  mm<sup>2</sup>), APDs were studied, devoting particular care to the radiation tolerance of these devices.

In the forward and backward end-caps, due to the high expected rate and other requirements, vacuum phototriodes (VPT) were the choice. Such devices, which have one dynode, exhibit only weak field dependence, and have high rate capabilities, absence of nuclear counter effect and radiation hardness.

### **5. Characterization of Avalanche Photodiodes for large detectors: procedures and results**

As discussed in the previous Sections, the construction of a large electromagnetic calorimeter based on Avalanche Photodiodes as readout devices may require a large number (in the order of  $10^3$ - $10^5$ ) of individual APDs to be tested and characterized, after the

R&D phase has successfully contributed to produce a device compliant with the specifications required by the experiment. Not only the devices have to be checked for their possible malfunctioning, but to minimize the energy resolution for high energy electromagnetic showers, it is important to obtain and assure a relative energy calibration between the different modules into which the calorimeter is segmented. The uncertainty in the inter-module calibration contributes to the constant term in the overall energy resolution, which becomes most significant at high energy. An additional motivation to have a good module-to-module calibration comes from the possibility to implement on-line trigger capabilities, especially for high energy and jet events. In such case, it is mandatory to adjust the individual gains of the various channels within a few percent.

For all such reasons, a massive work is usually required to choose the optimal APD bias for each individual device. Such massive production tests allow also to check the functionality of the device under test and the associated preamplifier, prior to mounting them in the detector. Mass production tests carried out in the lab prior to installation usually consist of measurements of the gain versus voltage dependence of each APD at fixed and controlled temperature, and in the determination of the required voltage to reach a uniform gain for all the devices.

Several properties may be measured during this screening operation, depending on the amount of information required, the desired precision and the amount of time at disposal to carry out all the required operations in a reasonable time schedule. If the device under consideration originates from a stable production chain at the manufacturer's site, as it is usually for APDs which have been in use for several applications, a complete set of characterization procedures may be carried out only for limited samples of devices. These may include the evaluation of the quantum efficiency, of the excess noise factor, of the capacitance, dark current and gain uniformity over the APD surface, as well as the temperature dependence of the gain curve in a wide range of temperatures (Karar, 1999). Massive tests, to be carried out on each individual APD, at least require the measurement of the gain-bias voltage curve at one or more temperatures, close to the operational one, and (possibly) the measurement of the dark current at different gain values. From the measured data one can extract the bias voltage required to match a fixed value of the gain, and the voltage coefficient.

The basic equipment to carry out such tests includes a system to maintain and measure the APD temperature while performing the measurements (usually within 0.1 °C), a pulsed light source (for instance a pulsed LED in the appropriate wavelength region), the front-end electronics and some acquisition system to store the data for further analysis. Due to the large number of devices usually under test, a suitable procedure must be designed, which tries to minimize as much as possible the time required to carry out a complete scan. As an example, the test of several APDs (8-32) at the same time may be planned with a proper choice of the readout system. Moreover, bias voltage may be software controlled together with acquisition, thus allowing to carry out automatic measurements in controlled steps of bias voltage.

Fig.2 shows an example of a typical gain curve obtained during the characterization of a large number of Hamamatsu S8148 APDs within the ALICE Collaboration (Badalà, 2008).

The output signal was measured for different values of the bias voltage, from 50 V (where a plateau is expected, corresponding to unitary gain) to about 400 V. The data were fitted by the function:

$$M(V) = p_0 + p_1 \exp(-p_2 V) \quad (4)$$

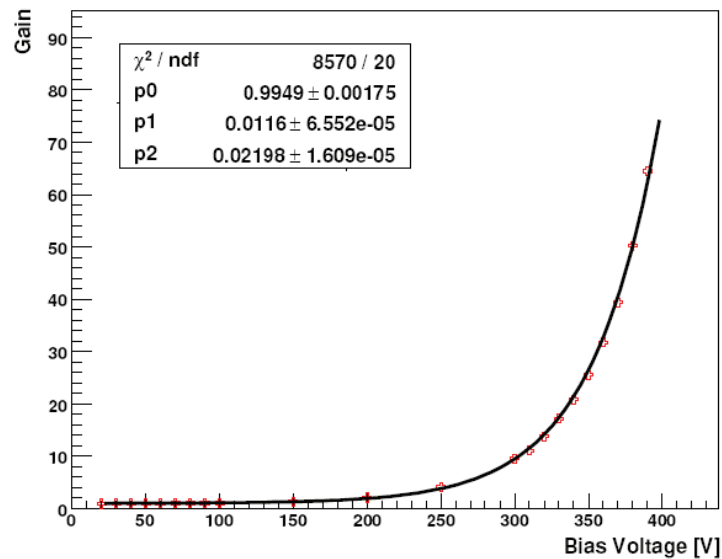


Fig. 2. Gain curve as a function of the APD bias voltage, for one of the Hamamatsu S8148 employed in the ALICE electromagnetic calorimeter. A common gain of 30 is usually set for all the modules.

in order to extract the coefficients  $p_0$ ,  $p_1$ ,  $p_2$  and thus determine the voltage  $V_{30}$  at which the gain equals  $M=30$ , which is the required value in the ALICE EMCal.

The relative change in the gain with the bias voltage is an important parameter to extract from such measurements, especially in the region where the APD will work. Fig.3 reports one of such results, showing a value of 2.3 %/V at  $M=30$ .

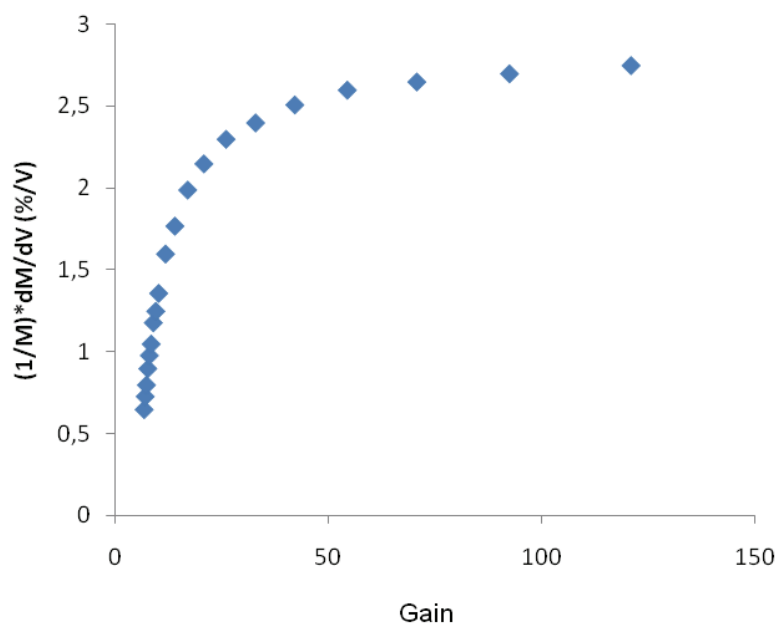


Fig. 3. The relative change in the APD gain is here reported at different values of the gain.

Due to the strong dependence of the APD gain from the temperature, the investigation of the gain versus temperature is an important issue of the characterization phase, at least for subsamples of the complete set of devices. Gain curves have to be measured for different



values of the temperature – spanning the region of interest – in order to extract a temperature coefficient. Fig.4 shows an example of a set of different gain curves measured in the range 21 to 29 °C, for the Hamamatsu S8148 APDs.

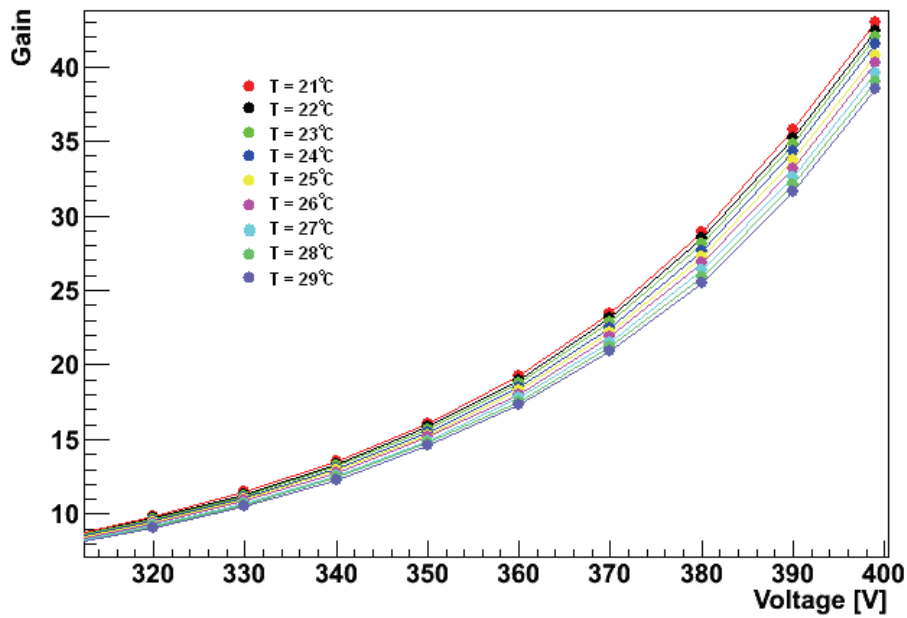


Fig. 4. Gain curves measured at different temperatures.

This or similar sets of measurements allow to extract the gain versus temperature dependence (Fig.5) and finally a value of the temperature coefficient, which decreases with the temperature, as shown in Fig.6.

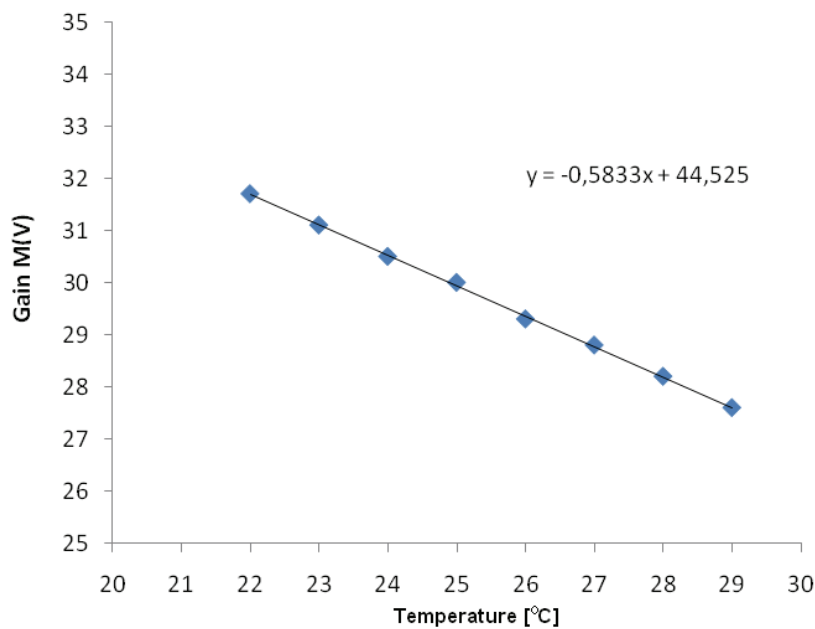


Fig. 5. APD gain as a function of the temperature.

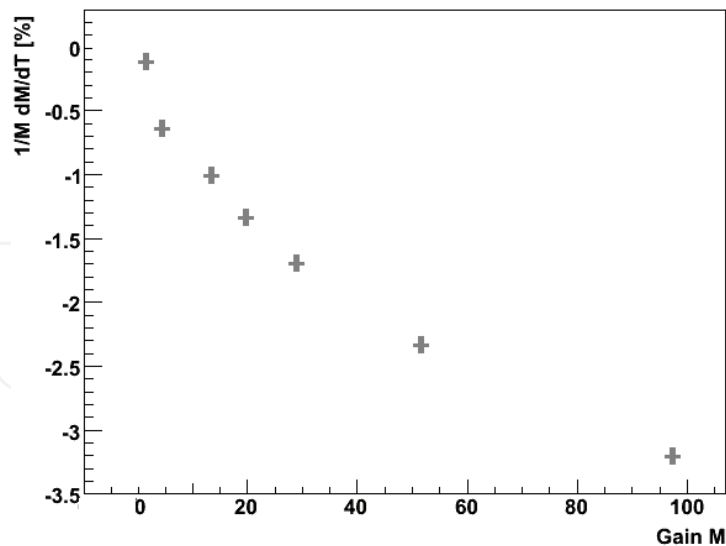


Fig. 6. Temperature coefficient of the APD gain, reported as a function of the APD gain.

All these procedures allow to classify the individual devices into different categories (for instance according to the voltage required to match a given gain, or to the temperature coefficient) for the sake of response uniformity, and to reject APDs with inadequate performance. Carrying out systematic characterization of a large number of individual devices permits to investigate statistical distribution of several quantities of interest, and establish classification criteria, to be used for the next samples. As an example, Fig.7 shows the distribution of the bias voltages required to have a common gain ( $M=30$ ) in a set of 1196 APDs which were used in one of the super-module of the ALICE electromagnetic calorimeter.

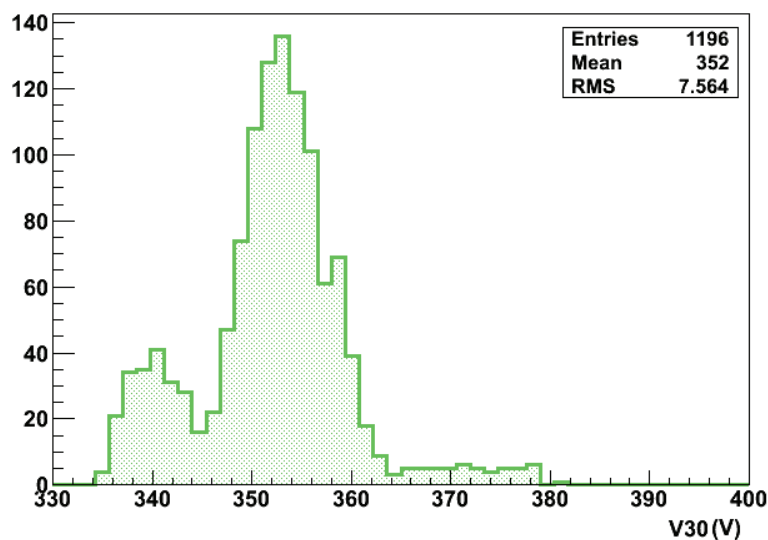


Fig. 7. Statistical distribution of the APD bias voltages required to match a common gain  $M=30$ , for a set of 1196 devices employed in one of the super-modules of the ALICE calorimeter.

While the distribution shows clearly the presence of two populations (due to different production lots), all devices showed a bias voltage smaller than 400 V, which was the limit set by the electronic circuitry to power the APD with a sufficient resolution. Fig.8 shows also

the distribution, for the same set, of the voltage coefficient, which has an average value of 2.3%/V, with an RMS in the order of 0.08 %/V.

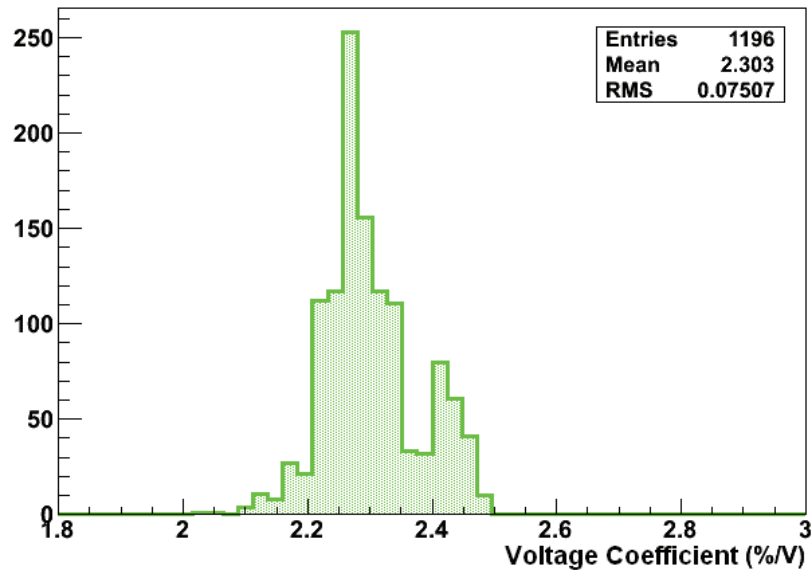


Fig. 8. Statistical distribution of the voltage coefficients, for the same set of 1196 APDs.

## 6. Extraction of amplitude and time information: traditional methods and alternative approaches

The output signal from Avalanche Photodiodes needs to be analyzed to extract as much as possible the information contained. Particularly relevant are of course the amplitude information, related to the amount of energy deposited in the individual module, and the timing information associated to it. The procedures to extract such information are not trivial, especially when analyzing events which span a large dynamical range, as it is the case for electromagnetic calorimeters in high energy experiments. In such a case, various algorithms have been developed and used, whose relative merits may be compared according to the precision and CPU time required. Even methods based on neural network topologies may be implemented and applied to simulated and real data.

With reference to Fig.9, which shows a typical signal, as sampled by a flash ADC, the shape of the signal may be fitted by a Gamma function

$$\text{ADC}(t) = \text{Pedestal} + A^{-n} x^n e^{-n(1-x)}, \quad x = (t-t_0)/\tau \quad (5)$$

where  $\tau = n \tau_0$ ,  $\tau_0$  being the shaper constant, and  $n \sim 2$ .

Such fit procedure is certainly able to provide reliable values of the amplitude  $A$  and time information  $t_0$  in case of large-amplitude signals, for which the number of time samples is relatively high (larger than 5-7). However, there are two main drawbacks inherent to this method: the algorithm is relatively slow, if one considers that it has to be applied to a large number of individual modules on an event-by-event basis, which is dramatic especially for on-line triggering. Secondly, in case of signals with very low amplitudes, the fit quite often provides unreliable values, since the signal shape is no longer similar to a Gamma function. For such reasons, alternative approaches have been tested and compared to the standard fitting procedure: fast fitting methods, peak analysis and so on. Here we want to show an example based on a neural network approach, which was recently tested on a sample of

LED calibration data obtained for a large number (a few thousands) of channels in the ALICE electromagnetic calorimeter.

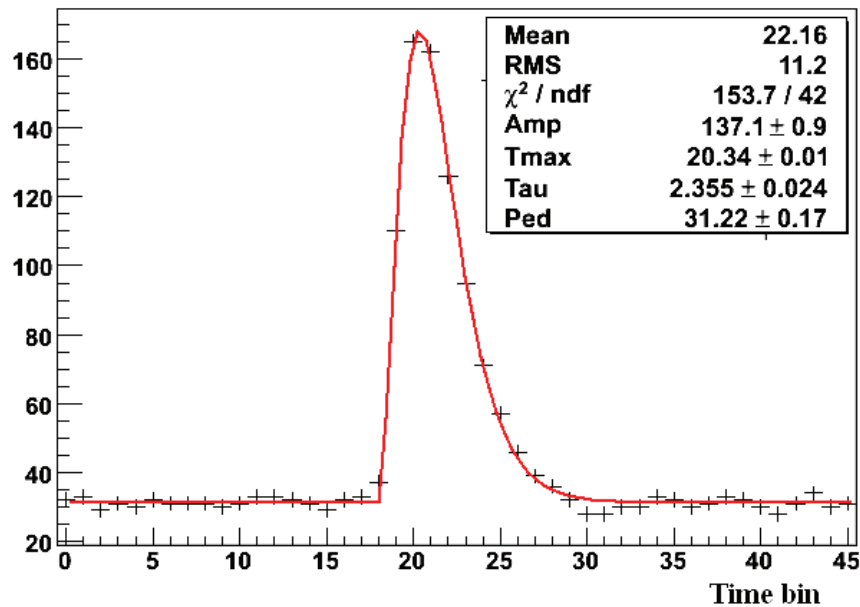


Fig. 9. Shape of the signal, as extracted from a sampling ADC.

In order to prepare a data sample which exhibits its maximum at different times, as it could happen for real data, the LED signal was shifted in time every 100 events.

Also the amplitude distribution is very broad, in order to span a region as large as possible, similarly to real data. This was due to the inevitable difference in the distribution of the light signal to the different modules. As a result, Figs.10 and 11 show two examples of a high amplitude (number of time samples = 12) and a low amplitude signal (number of time samples = 6). All the data were processed with the standard fit algorithm, which provided the reference for the learning phase in the neural network approach.

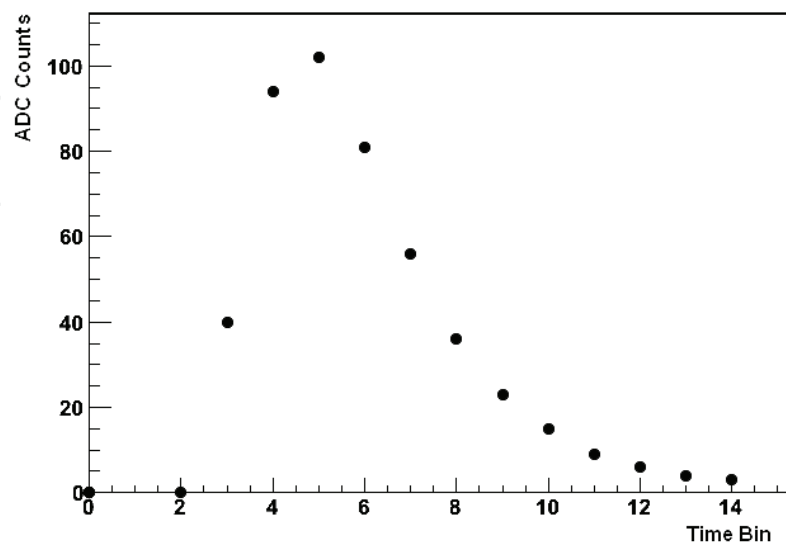


Fig. 10. An example of a high amplitude signal, including 12 time samples.

A feedforward multilayered neural network (Bishop, 1995) consists of a set of input neurons, one or more hidden layers of neurons, a set of output neurons, and synapses connecting each layer to the subsequent layer. The synapses connect each neuron in the first layer to each neuron in the hidden layer and each neuron of the hidden layer to the output (Fig.12). Several topologies may be chosen, as far as the number of input neurons and hidden layers are concerned.

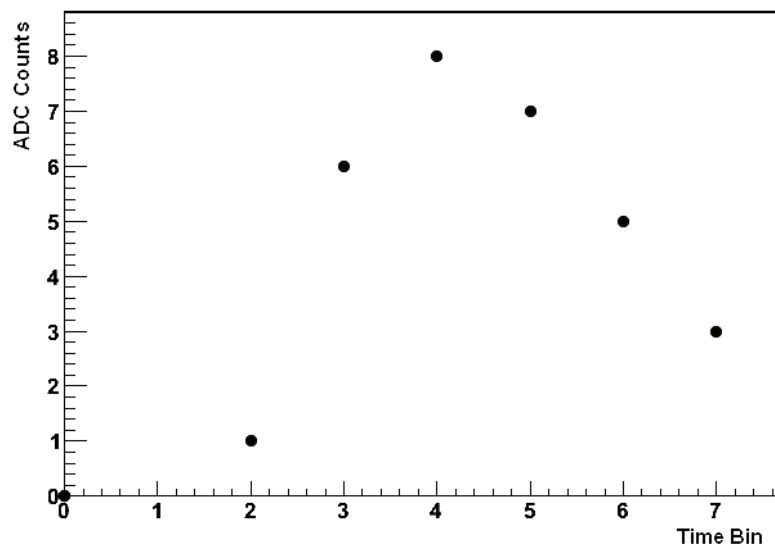


Fig. 11. An example of a low amplitude signal, including only 6 time samples.

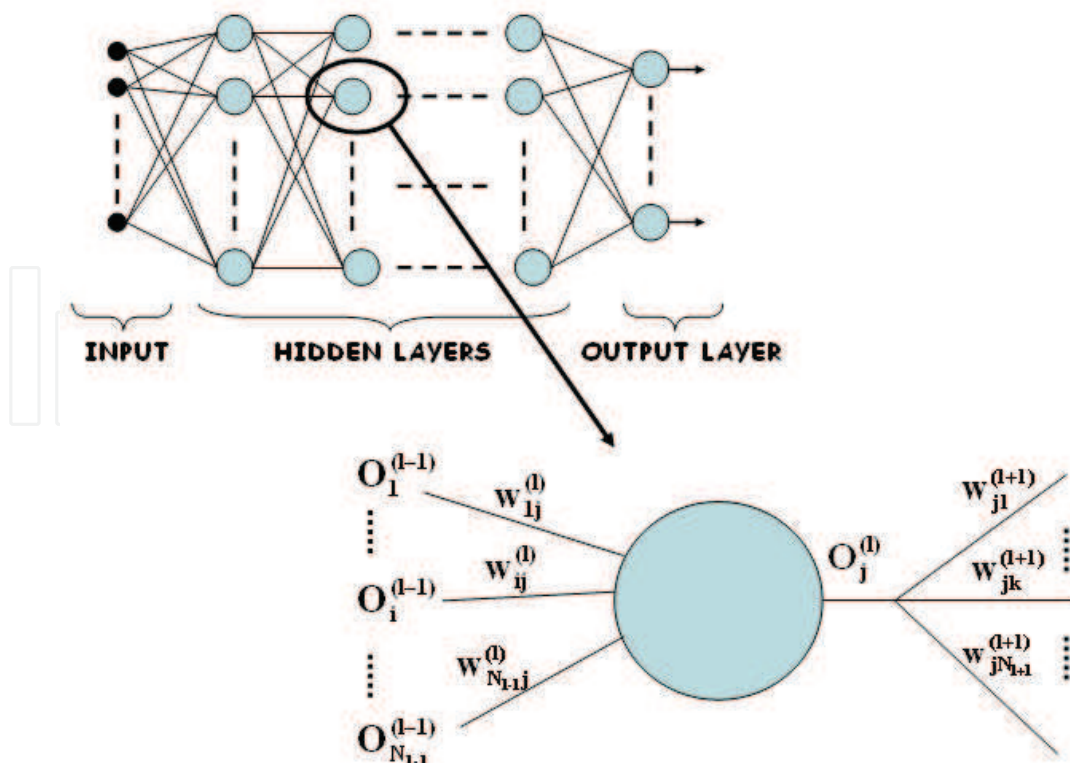


Fig. 12. Schematic layout of a neural network.



The signal provided by the  $j$ -th neuron of the  $l$ -th layer is given by the linear combination of the neuron input values, where the  $w$ 's are the weights:

$$a_j = \sum_{i=1}^{N_{l-1}} w_{ij}^{(l)} O_i^{(l-1)}$$

A backpropagation algorithm was used in the learning phase, in order to modify the initial values of the weights and minimize the error function:

$$E = \frac{1}{2} \sum_{p=1}^{N_p} \sum_{j=0}^{N_o} [y_{jp} - O_{jp}^N]^2$$

Best results were obtained in this case with 5 input neurons (the 5 values of the signal amplitude closest to the maximum), 10 hidden neurons and 2 output neurons (the amplitude and the time of the signal peak). Fig.13 shows the minimization of the error function with the number of epochs employed in the learning and testing phases.

Figs.14 and 15 show the distributions of the differences between the reference values (provided by the Gamma-fit) and the output values from the neural network, both for the amplitude and the time. An RMS of 0.26 ADC channel was obtained for the signal amplitude, while a value of 0.007 channel bin (corresponding to 700 ps) was obtained for the time.

Such performance was compared to more traditional methods, based on fast fitting procedures or peak analysis methods, and it was shown that after a proper training phase, comparable results may be in principle obtained by a neural network, with a reduced CPU time.

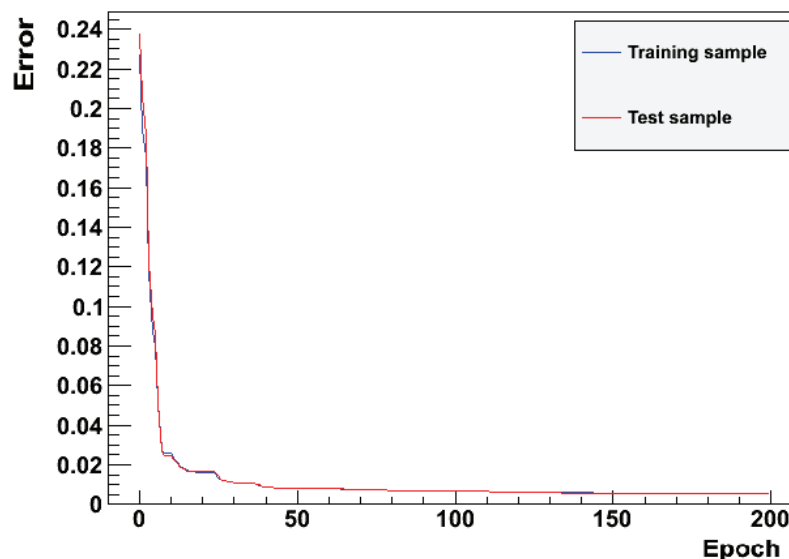


Fig. 13. Minimization of the error function with a neural network.

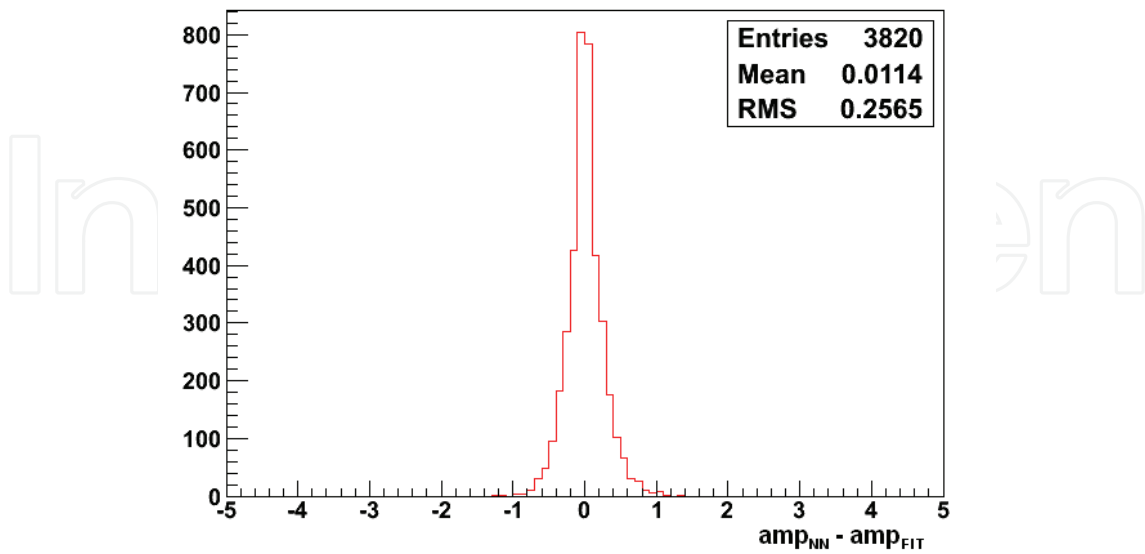


Fig. 14. Distribution of the differences between the “true” value (provided by the fit with a Gamma-function) and the value provided by the neural network, in case of the signal amplitude.

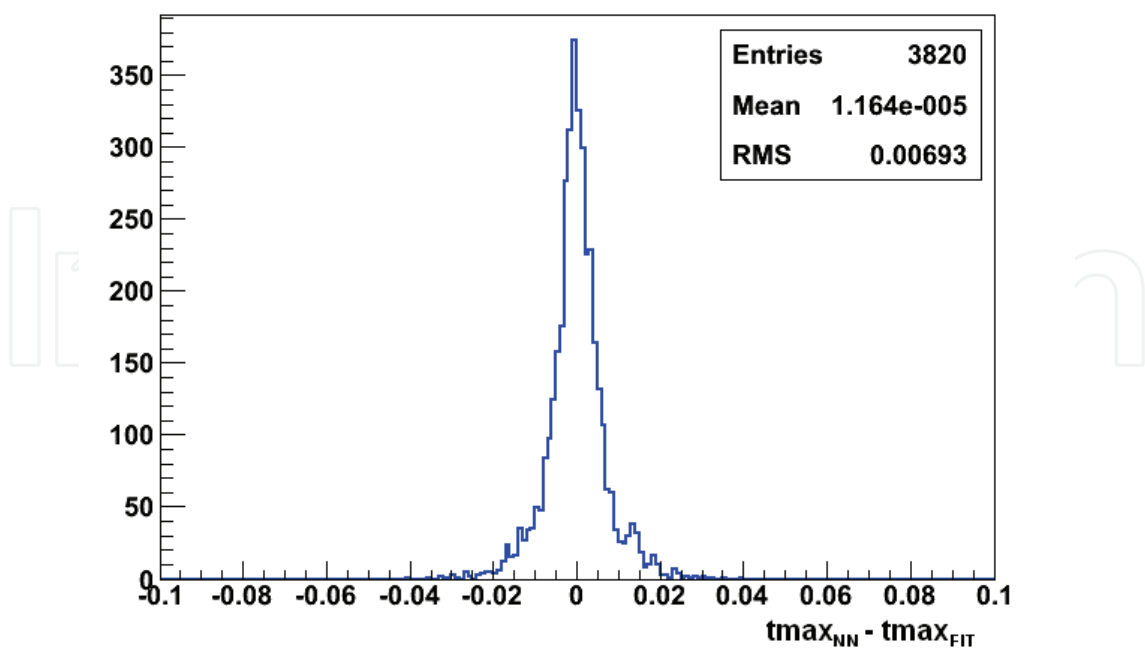


Fig. 15. As for fig.14, for the time information.

## 7. Conclusion

After several years of R&D work, Avalanche Photodiodes have proved to be a mature technology to be routinely employed in the design and construction of large high-energy calorimeters for the readout of the scintillation light produced in the individual calorimeter cells. The use of APDs in high energy electromagnetic calorimetry has required large efforts from both physics Laboratories and Industries in order to improve several aspects allowing an efficient usage of these devices in particle detectors. As a result of these combined efforts, several devices have been developed which have a reasonable sensitive area, a suitable spectral sensitivity and a good resistance to radiations. Different experiments incorporating one or more electromagnetic calorimeters in their setup make now use of a large number (in the order of  $10^5$ ) of these devices with good results, and additional projects are looking forward to this solution. Several progresses are however possible along different directions. One aspect is certainly related to the increase in the sensitive area of the individual devices, without losing any advantage originating from their intrinsic properties. This will allow a more efficient coupling of APDs to the scintillation crystals. Optimization of the spectral response in connection with the choice of the scintillation material is certainly another direction where some development could be expected in the next future. Additional improvements could come from the monitoring and control of such devices, in order to optimize and stabilize their gain as a function of the bias voltage and of the operating temperature.

## 8. References

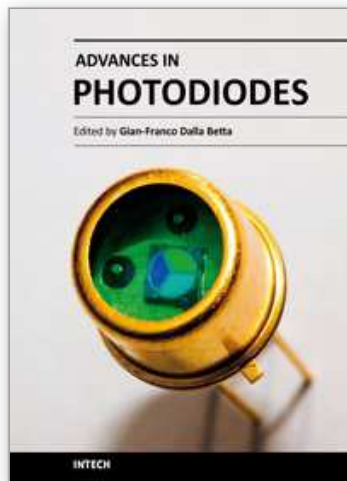
- Aamodt, K. et al., The ALICE Collaboration (2008). The ALICE detector at LHC, *Journal of Instrumentation* 3, S08002
- Anzivino, G. et al. (1995). *Review of the hybrid photo diode tube (HPD) an advanced light detector for physics*, Nuclear Instruments and Methods A365, 76-82
- Badalà, A. et al.(2008). *Characterization of Avalanche Photodiodes for the electromagnetic calorimeter in the ALICE experiment*, Nuclear Instruments and Methods A596, 122-125
- Badalà, A. et al.(2009). *Prototype and mass production tests of avalanche photodiodes for the electromagnetic calorimeter in the ALICE experiment at LHC*, Nuclear Instruments and Methods A610, 200-203
- Barlow, R.J. et al.(1999). *Results from the BABAR electromagnetic calorimeter beam test*, Nuclear Instruments and Methods A420, 162-180
- Bishop, C.M. (1995). *Neural Networks for Pattern Recognition*, Clarendon, Oxford
- Chartrchyan, S. et al., The CMS Collaboration (2008). The CMS detector at LHC, *Journal of Instrumentation* 3, S08004
- Erni, W. et al., The PANDA Collaboration (2008). *Technical Design Report*, arXiv :0810.1216v1
- Fabjan, C.W. & Gianotti, F. (2003), *Review of Modern Physics* 75,1243-1286
- Lorenz, E. et al. (1994), *Fast readout of plastic and crystal scintillators by avalanche photodiodes*, Nuclear Instruments and Methods A344, 64-72
- Karar, A.; Musienko, Yu. & Vanel, J.Ch. (1999), *Characterization of Avalanche Photodiodes for calorimetry applications*, Nuclear Instruments and Methods A428,413-431

Musienko, Yu. (1992), The CMS electromagnetic calorimeter, *Nuclear Instruments and Methods A* 494, 308-312

Wigmans, R. (2000), *Calorimetry: Energy Measurements in Particle Physics*, University Press, Oxford

IntechOpen

IntechOpen



### **Advances in Photodiodes**

Edited by Prof. Gian Franco Dalla Betta

ISBN 978-953-307-163-3

Hard cover, 466 pages

**Publisher** InTech

**Published online** 22, March, 2011

**Published in print edition** March, 2011

Photodiodes, the simplest but most versatile optoelectronic devices, are currently used in a variety of applications, including vision systems, optical interconnects, optical storage systems, photometry, particle physics, medical imaging, etc. *Advances in Photodiodes* addresses the state-of-the-art, latest developments and new trends in the field, covering theoretical aspects, design and simulation issues, processing techniques, experimental results, and applications. Written by internationally renowned experts, with contributions from universities, research institutes and industries, the book is a valuable reference tool for students, scientists, engineers, and researchers.

#### **How to reference**

In order to correctly reference this scholarly work, feel free to copy and paste the following:

Paola La Rocca and Francesco Riggi (2011). The Use of Avalanche Photodiodes in High Energy Electromagnetic Calorimetry, *Advances in Photodiodes*, Prof. Gian Franco Dalla Betta (Ed.), ISBN: 978-953-307-163-3, InTech, Available from: <http://www.intechopen.com/books/advances-in-photodiodes/the-use-of-avalanche-photodiodes-in-high-energy-electromagnetic-calorimetry>

**INTECH**  
open science | open minds

#### **InTech Europe**

University Campus STeP Ri  
Slavka Krautzeka 83/A  
51000 Rijeka, Croatia  
Phone: +385 (51) 770 447  
Fax: +385 (51) 686 166  
[www.intechopen.com](http://www.intechopen.com)

#### **InTech China**

Unit 405, Office Block, Hotel Equatorial Shanghai  
No.65, Yan An Road (West), Shanghai, 200040, China  
中国上海市延安西路65号上海国际贵都大饭店办公楼405单元  
Phone: +86-21-62489820  
Fax: +86-21-62489821



© 2011 The Author(s). Licensee IntechOpen. This chapter is distributed under the terms of the [Creative Commons Attribution-NonCommercial-ShareAlike-3.0 License](#), which permits use, distribution and reproduction for non-commercial purposes, provided the original is properly cited and derivative works building on this content are distributed under the same license.

IntechOpen

IntechOpen